GEOPHYSICAL RESEARCH LETTERS, VOL. 28, NO. 18, PAGES 3481-3484, SEPTEMBER 15, 2001

Heat transport, deep waters, and thermal gradients: Coupled simulation of an Eocene Greenhouse Climate

Matthew Huber and Lisa Cirbus Sloan

Earth Sciences Department, University of California, Santa Cruz

Abstract. For the first time, a coupled general circulation model with interactive and dynamical atmospheric, oceanic, and sea-ice components, is used to simulate an Eocene (∼50 Ma) "greenhouse" climate. We introduce efficient ocean spin-up methods for coupled paleoclimate modeling. Sea surface temperatures (SSTs) and salinities evolve unconstrained, producing the first proxy data-independent estimates for these Eocene climate parameters. Tropical and extratropical model-predicted SSTs are warmer than modern values, by 3 and 5°C, respectively. Salinity-driven deep water formation occurs in the North Atlantic and Tethys. The zonal average overturning circulation is weaker than modern. Eocene ocean heat transport is 0.6 PW less than modern in the Northern Hemisphere and 0.4 PW greater in the Southern Hemisphere. The model–predicted near–modern vertical and meridional Eocene temperature gradients imply that the dominant theory for maintaining low gradients—increased ocean heat transport—is incorrect or incomplete and other mechanisms should be explored.

Introduction

Understanding the interaction of all components of the Earth System in past, warm, "greenhouse" climates is a principal goal of paleoclimatology. One of the most intriguing of these greenhouse periods is the Eocene (56-33 Ma), for which proxy data predict warm (6-12°C) deep ocean and polar temperatures, near-modern (23-27°C) tropical sea surface temperatures (SSTs) [*Zachos et al.*, 1994; *Crowley and Zachos*, 2000], and higher-than-modern greenhouse gas levels (pCO$_2$ 400-4000 ppm) [*Pearson and Palmer*, 2000]. This combination of smaller temperature gradients and higher pCO$_2$ has only been explained by invoking oceanic heat transport much greater than present values [2-3x modern, *Sloan et al.*, 1995; *Huber and Sloan*, 1999]—a solution without any known mechanism.

Consequently, attention has focused on modeling paleo-ocean circulations and, especially, on constraining ocean heat transport in past greenhouse climates [*Schmidt and Mysak*, 1996; *Lyle*, 1997; *Brady et al.*, 1998]. While the formation of warm salty deep water (WSDW) has frequently been suggested as the cause of warm polar temperatures and increased ocean heat transport [*Brass et al.*, 1982], these conjectures have not been supported by theory [*Sloan et al.*, 1995], uncoupled ocean modeling [*Brady et al.*, 1998], or simplified dynamic coupled modeling [*Saravanan and McWilliams*, 1995]. Previous attempts to address the question of Eocene ocean heat transport and temperature gradients have been limited by their inability to properly represent feedbacks between ocean circulations—the thermohaline component in particular—and the atmosphere [*Sloan and Rea*,1996]. Below, we introduce a technique for simulating past climates with a coupled general circulation model (CGCM) and address key climate questions that have not previously been treated in a coupled framework with realistic Eocene boundary conditions: (1) Are meridional overturning circulations weaker in an Eocene climate? (2) Where does deep water form, and is the circulation dominated by temperature or salinity gradients (thermohaline or halothermal)? (3) What is the oceanic heat transport? (4) Can small thermal gradients be maintained by a coupled model?

Paper number 2001GL012943.
0094-8276/01/2001GL012943$05.00

Model Description and Methodology

Paleoclimate modeling with CSM

We simulate Eocene climate with the Climate System Model (CSM) developed at the National Center for Atmospheric Research (NCAR). CSM version 1 (v.1) is described and validated for modern conditions in *Boville and Gent* [1998] and references therein. Our results are produced with an updated version, 1.4, described for a modern and a Cretaceous experiment in *Otto-Bliesner and Brady* [2001] and *Otto-Bliesner et al.* [Otto-Bliesner, B., E. Brady and C. Shields, submitted, J. Clim.], and briefly below. The atmospheric and land models are the Community Climate Model (CCM) 3.6 and the Land Surface Model (LSM) 1.2 at T31 resolution. These are coupled to NCAR's Ocean Model (NCOM) 1.5 and the Community Sea Ice Model (CSIM) 2.2. The latter models are on a stretched grid with .9° equatorial and 1.8° high latitude meridional grid spacing; zonal resolution is 3.6°. Components are connected through the Flux Coupler v. 4. The major differences from CSM v.1 are (1) better resolved tropical ocean circulations and thermocline structure, and (2) improvements in conservation properties of Flux Coupler interpolation between component models.

The main limitation in performing fully coupled paleoclimate simulations is the deep ocean circulation. The simulation length needed to equilibrate the deep ocean (O 2000 yrs) can be computationally infeasible and most CGCMs require "flux corrections" to maintain present day conditions. It is problematic to apply flux corrections in the distant past because the state toward which the model would be "corrected" is unknown. The CSM is one of the few CGCMs that does not require flux corrections for the modern day, thus it satisfies a necessary condition for paleoclimate simulation.

To demonstrate the possibility of convergence on a realistic coupled solution from rough knowledge of initial and boundary conditions, we first perform an iterative modeling

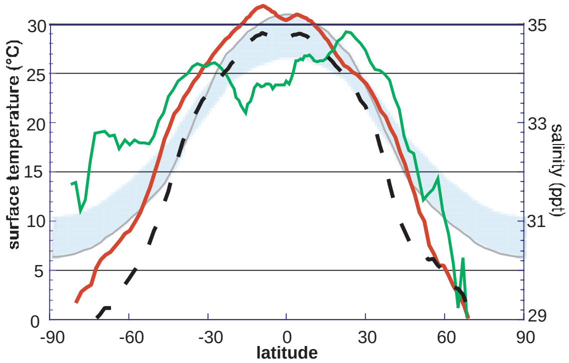

Figure 1. Zonal, annual mean SST and salinity. The Eocene simulation is initialized with SSTs (grey line) and equilibrates with the SSTs (red line) and salinity (green line) above. The approximate range of early-to-mid Eocene SSTs from proxies including possible biases are indicated in blue [estimates from *Zachos et al.*, 1994; *Crowley and Zachos*, 2000; *Huber and Sloan*, 2000]. Degraded modern simulated SSTs are shown with a dashed line.

sequence for a "degraded" present day case. Degraded denotes that we have filtered modern day boundary conditions to a level of detail similar to that available for the Eocene. The degraded present case has simplified bathymetry and soil properties, and we have removed an albedo tuning that made Antarctic/Siberian snow more reflective. Analogous simplifications and removal of tuning performed in the degraded present case are applied in the Eocene experiment by necessity. In the Eocene simulation, we incorporate realistic, "best guess" Eocene bathymetry, topography, land surface conditions, $p\mathrm{CO_2}$ (560 ppm), and vegetation as boundary conditions [described in *Sewall et al.*, 2000].

Iterative procedure and validation

We employ an iterative method to reach a climatic equilibrium for conditions extremely different from those of today. This method is akin to, but different than, those discussed by *Vavrus et al.* [2000] and *Otto-Bliesner et al.* [submitted, J. Clim.]. Below we outline the method to accelerate convergence of the deep ocean to an equilibrium state and briefly discuss results from the degraded present day case.

(1) CCM and LSM are driven by fixed, zonally constant, SSTs. For the degraded present case, the monthly varying fixed SSTs are taken from the *Shea et al.* [1990] dataset. We begin in this way because Eocene conditions (the focus of this study) are known well enough to characterize zonal-annual mean SSTs and some degree of seasonal variability, but not east-west SST variations.

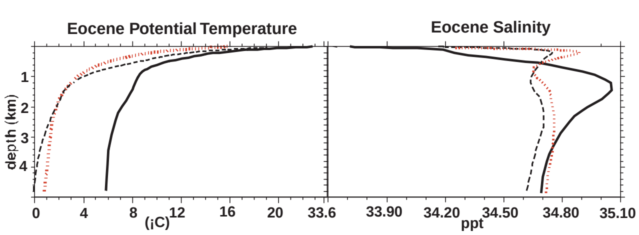

Figure 2. The equilibrated globally averaged vertical profiles of potential temperature (left) and salinity (right) for the Eocene case (black solid line) and degraded modern (black dashed line), and modern observed (red dashed line).

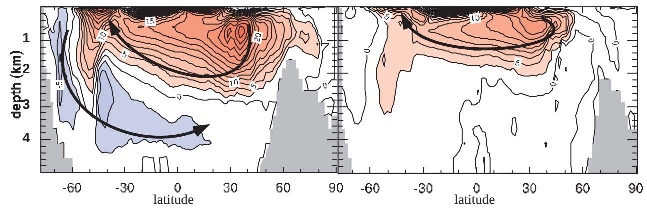

Figure 3. Zonal, annual average meridional overturning streamfunction (in Sv). The degraded modern (left) is close to standard present day CSM simulations. The Eocene case (right) is substantially weaker.

(2) This spun up atmosphere/land surface is coupled to the other components of CSM. Initial ocean conditions for the degraded present case are zonally averaged temperature and salinity taken from *Levitus and Boyer* [1994] and *Levitus et al.* [1994] and a state of rest. Initially, sea-ice is located in regions with SSTs less than -1.8°C (and a "ramp" function between -0.8 and -1.8°C). After 50 years, regions of deep convection become well established, sea-ice is equilibrated, and the wind-driven ocean circulation is vigorous. Because initial conditions are zonally constant, there is, at first, no preference for North Atlantic sinking in the present day case; sinking occurs equally in the North Atlantic and Pacific and to a lesser degree in the Southern Ocean.

(3) NCOM and CSIM are driven by CCM/LSM output from the final 5 years of the coupled simulation (2). They are integrated for 20 years with deep ocean acceleration, i.e., 1000 Deep Water Years (DWY) (described by *Danabasoglu et al.* [1996] except with 50x tracer time steps and no momentum acceleration) and 10 years unaccelerated. In this phase of the present day experiment, Antarctic bottom water formation slows, Antarctic Circumpolar Current (ACC) transport decreases, and both Northern Hemisphere sinking modes increase in strength.

(4) In the next fully coupled iteration, CCM and LSM are initialized with conditions from the end of (2), and NCOM and CSIM begin from the end of (3). With the deep ocean further equilibrated, the North Atlantic sinking mode becomes dominant and meridional overturning, centers of deep convection, and key global and regional properties converge on values (Table 1) similar to reference CSM simulations, e.g. *Boville and Gent* [1998] and *Bryan* [1998]. Temperature and salinity trends are small (Table 1).

The simulation's major weakness is too-weak formation of Antarctic Bottom water (3 Sv) and a sluggish ACC (85 Sv). When integrated for long periods, CSM v.1 tends toward overly-strong Antarctic Bottom water formation and ACC transport as described in *Bryan* [1998]. Based on *Bryan* [1998], our interpretation is that these features are sensitive to model formulation (especially sea-ice and albedo feedbacks) and spin-up procedures. Sea-ice was not likely to have been present in the warm polar Eocene climate and does not play an important role in our results described below, so this sensitivity affects our Eocene results minimally. Importantly, the degraded present case required only two fully coupled integrations with one intervening 1000DWY accelerated, uncoupled integration, in order to establish a global ocean circulation close to observed.

The Eocene simulation is initialized in (1) with SSTs shown in Figure 1 smoothly fit to a deep ocean temperature of 6°C, and salinity initially set to a global average value of 34.7 ppt. The Eocene simulation is spun up with

Table 1. Summary of ocean model results

	Present	Eocene
Volume Average T	3.28	8.115°C
Volume Average S	34.670	-34.771 ppt
Volume Average T Trend[a]	-.068	.004°C/Century
Volume Average S Trend	.0008	-.0004 ppt/Century
NADW formation rate[b]	22	10 Sv
Tethyan DW formation rate	—	8 Sv
ACC volume transport	83	7 Sv
North Atlantic Overturning	25	12.5 Sv

[a]Temperature and salinity trends calculated by least squares fits over the last 30 years.

[b]Formation rates are evaluated by the volume flux through a depth and location representative of the watermass.

the steps outlined above but with an additional iteration (repeat of Steps 3 and 4) needed to demonstrate convergence on a stable climate. The total length of the integration is 2185 DWYs, the temperature trend for the last 30 years is small (Table 1), and there was little significant difference between the results of (4) and (6), indicating convergence (not shown). The iterative method is robust and leads to an equilibrated coupled simulation that produces present climate well in the degraded case and a stable and convergent solution in the Eocene case. Means of the last five years are discussed below.

Eocene Results

Our Eocene simulation produces average SSTs and deep ocean temperatures that are 3 to 7°C warmer than the degraded present case (Figures 1, 2). Seasonal sea-ice occurs in the Labrador Sea, in several North Pacific grid cells, and in a small region along the Antarctic margin near Australia (not shown). The Arctic Ocean, which is not connected to the global oceans in this simulation, is ice-covered on a seasonal basis. Globally averaged vertical temperature gradients are little changed from modern (Figure 2).

In all previous Eocene ocean modeling, salinity was fixed or determined from modeled atmospheric surface water fluxes, with no opportunity for feedbacks. The more realistic treatment of freshwater fluxes in this study yields the result that the Southern Oceans and North Pacific are relatively fresh (~32 ppt) due to strong net precipitation; the North Atlantic and the northern reaches of Tethys are very saline, ~35.5 ppt and 36 ppt, respectively, and warm, 12-16°C (not shown).

We diagnose the location and depth of oceanic deep convection using mixed layer depth and an Ideal Age tracer. These diagnostics show that Intermediate/Deep water forms predominately in Tethys and the North Atlantic. Tethyan water penetrates to depths of ~2000 m and then flows into the Indian Ocean; North Atlantic water sinks to peak depths of ~3000 m, but the flow is predominately at ~2000 m and is directed into the Pacific and South Atlantic Oceans. The temperatures and salinities of these watermasses are (at depth) 9°C and 35.25 ppt, and 8°C and 35.0 ppt, respectively. These features make intermediate ocean depths more saline than in the present day case, while the global upper ocean is relatively fresh because of vigorous precipitation in the high latitude Pacific (Figure 2).

Whereas vigorous sinking in Tethys and the North Atlantic is associated with seasonal cooling, the sites of deep convection are dictated by large-scale salinities. We define this circulation as quasi-halothermal because the densest waters in the simulation are derived from the rapid sinking of warm, salty water masses, rather than the much fresher and cooler (by ~6°C) watermasses that are, in fact, displaced by these denser classes. The meridional overturning streamfunction in the Eocene case is substantially more sluggish than the present case (Figure 3). Model-predicted circulations are however, within 50% of those in the modern simulation.

In association with less vigorous meridional overturning circulation (Figure 3), oceanic heat transport is slightly reduced in the Eocene case relative to modern (Figure 4). Peak oceanic heat transport in the Eocene case is 1.6 PW in the Northern Hemisphere and 0.9 PW in the Southern Hemisphere. Eocene oceanic heat transport is therefore 0.6 PW less in the Northern Hemisphere than in the present day case, and 0.4 PW greater in the Southern Hemisphere. The majority of oceanic heat transport (80%) occurs in the Pacific, which is reasonable given its greater extent relative to the Atlantic during the Eocene [*Huber and Sloan*,1999].

Discussion and Conclusions

The higher pCO_2 used in the simulation is sufficient to remove most sea-ice and generate relatively warm high latitude SSTs but it also produces overly warm tropical SSTs relative to climate proxies [*Crowley and Zachos*, 2000]. The salinity distribution produced by the simulation suggests that existing proxy interpretations may, however, underestimate tropical SSTs and overestimate high latitude SSTs by ~4°C as suggested by *Huber and Sloan* [2000].

The model's tendency to produce near-modern gradients, with too-warm tropical SSTs and overly cool poles, when forced with higher-than-modern pCO_2 is consistent with results of all previous Eocene GCM studies with simplified ocean treatment [e.g., *Sloan and Rea*, 1996]. The lack of a marked decrease in SST gradients with realistic Eocene boundary conditions and full treatment of ocean circulation suggests it is unlikely that ocean currents were responsible for wide-spread polar warmth in the Eocene. Simulated Eocene currents do, however, generate some high latitude regional warming, much as they do today.

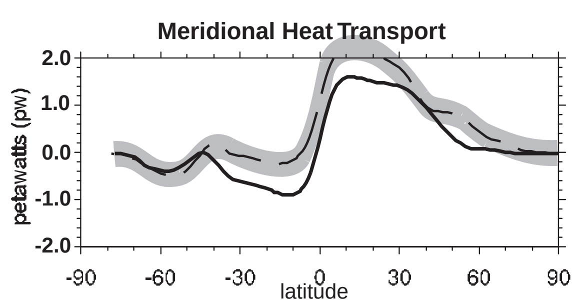

Figure 4. Meridional heat transports averaged over all ocean basins for the Eocene (solid line) and degraded modern (dashed line) cases. The grey zone is a qualitative error estimate, indicating the approximate uncertainty in heat transport introduced by the process of degradation (estimated by calculating the maximum transport difference between the degraded case and a reference run conducted at NCAR).

In the Eocene simulation, zonal average meridional overturning is reduced in intensity and depth relative to the modern day case. Consistent with the results of *Barron and Peterson* [1991], the locations of oceanic deep convection (the North Atlantic and Tethys) are predominantly dictated by salinity (and net evaporative) distributions. In addition, there is intermediate/deep water formation in the Southern Oceans (but not deep convection). There, wind-driven upwelling of cool (6°C), relatively fresh water leads to conversion of surface water into denser classes. These form a largely northward flowing component (depth ∼1000 m) with intermediate properties.

Taken together, these results are in general agreement with some interpretations of Eocene proxy data records in terms of the location, depth, temperature and salinity of deep water formation and qualitative measures of overturning [*Miller et al.*, 1987; *Kennett and Stott*, 1990; *Pak and Miller*, 1992]. Given the likelihood of multiple equilibria, however, we do not rule out other circulation modes [*Saravanan and McWilliams*, 1995]. A notable feature of the simulated deep water formation pattern is that North Atlantic Deep Water (NADW) forms even though the Isthmus of Panama is fully open and without input of saline water from Tethys, resolving an enigma posed in *Charisi and Schmitz* [1996].

Even though the model predicts production of relatively warm and salty deep water, our results do not support the hypothesis that increased ocean heat transport was responsible for Eocene climatic conditions. In keeping with theory and simplified coupled model studies [e.g., *Saravanan and McWilliams*, 1995], this simulation produces a more sluggish circulation, near-modern ocean heat transport and little-changed temperature gradients, in equilibrium with high than modern pCO_2. We believe that this simulation provides a useful baseline for comparison to climate/circulation proxies and a foundation for the development of greater understanding of the processes responsible for past warm climates.

The outstanding question in Eocene climate remains unanswered, what mechanism maintains warm poles without warming the tropics? Currently, we are comparing results of this simulation to those with varied Eocene initial and boundary conditions to explore the results' robustness and to test whether the match with temperature proxies can be improved or whether the ocean heat transport hypothesis should be finally rejected.

Acknowledgments. We thank B. Otto-Bliesner and E. Brady for pioneering paleoclimate modeling with CSM, and for invaluable assistance. We also thank reviewers T. Crowley and R. Oglesby for improving the manuscript. This research was supported by grants to L.C.S. from NSF: ATM9810799 and the D. and L. Packard Foundation. Computing was carried out at NCAR, supported by NSF.

References

Barron, E.J., and W.H. Peterson, The Cenozoic ocean circulation based on ocean general circulation model results, *Palaeogeogr. Palaeoclimatol. Palaeoecol., 83*, 1-28, 1991.

Boville, B.A., and P. R. Gent, The NCAR Climate System Model Version One, *J. Clim., 11*, 1115-1130, 1998.

Brass, G.W., J.R. Southam, and W.H. Peterson, Warm saline bottom water in the ancient ocean, *Nature, 296*, 620-623, 1982.

Bryan, F.O., Climate drift in a multicentury integration of the NCAR Climate System Model, *J. Clim., 11*, 1455-1471, 1998.

Charisi, S., and B. Schmitz, Early Eocene palaeoceanography and palaeoclimatology of the eastern North Atlantic: stable isotope results for DSDP Hole 550, in *Correlation of the Early Paleogene in Northwest Europe*, edited by R.W. O'B. Knox, R.M. Corfield, and R.E. Dunay, *Geol. Soc. Spec. Publ., 101*, 443-456, 1996.

Crowley, T.J., and J.C. Zachos, Comparison of zonal temperature profiles for past warm time periods, in Huber, B.T., K. G. MacLeod, and S. L. Wing, ed., *Warm Climates in Earth History*, Cambridge University Press, 2000.

Danabasoglu, G., J.C. McWilliams, and W.G. Large, Approach to equilibrium in accelerated global oceanic models, *J. Clim.*, *9*, 1092-1110, 1996.

Huber, M., and L.C. Sloan, Warm climate transitions: A general circulation modeling study of the Late Paleocene Thermal Maximum (∼56 Ma), *J. Geophys Res.*, *104*, 16,633-16,655, 1999.

Huber, M., and L.C. Sloan, Climatic responses to tropical sea surface temperature changes on a "greenhouse" Earth. *Paleoceanography*, *15*, 443-450, 2000.

Kennett, J.P., and L.D. Stott, Proteus and Proto-Oceanus: Paleogene oceans as revealed from Antarctic stable isotopic results, in Barker, P.F., Kennett, J.P., et al., *Proc. Ocean Drill. Program Sci. Results, 113*,865-880, 1990.

Levitus, S., and T.P. Boyer, Temperature, Vol. 4, *World Ocean Atlas* 1994, NOAA, 117 pp.

Levitus, S., R. Burgett, and T.P. Boyer, Salinity, Vol. 3, *World Ocean Atlas* 1994, NOAA, 99 pp.

Lyle, M., Could early Cenozoic thermohaline circulation have warmed the poles?, *Paleoceanography*, *12*, 161-167, 1997.

Miller, K.G., T.R. Janecek, M.R. Katz, and D.J. Keil, Abyssal circulation and benthic foraminiferal changes near the Paleocene/Eocene boundary, *Paleoceanography*, *2*, 741-761, 1987.

Otto-Bliesner, B.L., and E.C. Brady, Tropical Pacific variability in the NCAR Climate System Model. *J. Clim.*, in press 2001.

Pak, D.K., and K.G. Miller, Late Palaeocene to early Eocene benthic foraminiferal stable isotopes and assemblages: Implications for deepwater circulation, *Paleoceanography*, *7*, 405-422, 1992.

Pearson, P.N., and M.R. Palmer, Atmospheric carbon dioxide concentrations over the past 60 million years, *Science, 406*, 695-699, 2000.

Saravanan, R., and J.C. McWilliams, Multiple equilibria, natural variability, and climate transitions in an idealized ocean-atmosphere model, *J. Clim., 10*, 2296-2323, 1995.

Schmidt, G., and L. Mysak, Can increased poleward oceanic heat flux explain the warm Cretaceous climate?, *Paleoceanography, 11*, 579-593, 1996.

Sewall, J.O., L.C. Sloan, M. Huber, and S. Wing, Climate sensitivity to changes in land surface characteristics, *Global. Planet. Change, 26*, 445-465, 2000.

Shea, D.J., K.E. Trenberth, and R.W. Reynolds, A global monthly sea surface temperature climatology. NCAR/TN-345, pp. 167, 1990.

Sloan, L.C., and D.K. Rea, Atmospheric pCO_2 of the early Eocene: A general circulation modeling sensitivity study, *Palaeogeogr. Palaeoclimatol. Palaeoecol., 119*, 275-292, 1996.

Sloan, L.C., J.G. Walker, and T.C. Moore Jr., The possible role of oceanic heat transport in early Eocene climate, *Paleoceanography, 10*, 347-356, 1995.

Vavrus, S., R. Gallimore, and Z. Liu, A mixed-flux equilibrium asynchronous coupling scheme for accelerating convergence in ocean-atmosphere models, *Clim. Dyn., 16*, 821-831, 2000.

Zachos, J.C., L.D. Stott, and K.C. Lohmann, Evolution of early Cenozoic marine temperatures, *Paleoceanography, 9*, 353-387, 1994.

M. Huber, and L. C. Sloan , Earth Sciences Department, University of California, Santa Cruz, Santa Cruz, CA 95064. (e-mail: mhuber@es.ucsc.edu)

(Received January 31, 2001; revised April 20, 2001; accepted May 7, 2001.)